Influence of the Hofmeister Anions on Protein Stability As Studied by Thermal Denaturation and Chemical Shift Perturbation †

ARTICLE *in* BIOCHEMISTRY · FEBRUARY 2007

Impact Factor: 3.02 · DOI: 10.1021/bi0613426 · Source: PubMed

3 AUTHORS, INCLUDING:

Miquel Pons
University of Barcelona
170 PUBLICATIONS **3,305** CITATIONS
SEE PROFILE

Oscar Millet
Center for Cooperative Research in Biosciences
60 PUBLICATIONS **1,970** CITATIONS
SEE PROFILE

Article

Influence of the Hofmeister Anions on Protein Stability As Studied by Thermal Denaturation and Chemical Shift Perturbation

Xavier Tadeo, Miquel Pons, and Oscar Millet

Biochemistry, **2007**, 46 (3), 917-923 • DOI: 10.1021/bi0613426

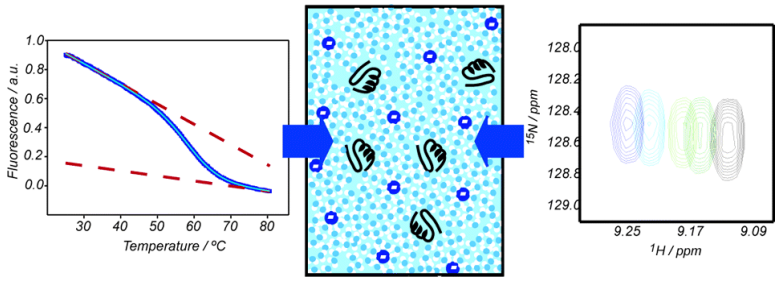

More About This Article

Additional resources and features associated with this article are available within the HTML version:

- Supporting Information
- Links to the 5 articles that cite this article, as of the time of this article download
- Access to high resolution figures
- Links to articles and content related to this article
- Copyright permission to reproduce figures and/or text from this article

View the Full Text HTML

Influence of the Hofmeister Anions on Protein Stability As Studied by Thermal Denaturation and Chemical Shift Perturbation†

Xavier Tadeo,‡ Miquel Pons,§ and Oscar Millet*,‡

Structural Biology Unit, CIC bioGUNE, Bizkaia Technology Park, Building 801A, 48160 Derio, Spain, Laboratory of Biomolecular NMR, Institute for Research in Biomedicine, Parc Científic de Barcelona, Josep Samitier 1-5, 08028 Barcelona, Catalonia, Spain, and Departament de Química Orgànica, Universitat de Barcelona, Martí i Franquès 1-5, 08028 Barcelona, Catalonia, Spain

Received July 3, 2006; Revised Manuscript Received November 16, 2006

ABSTRACT: The influence of external cosolutes on the thermal stability of the B1 domain of protein L (ProtL) has been studied by circular dichroism, fluorescence spectroscopy, and differential scanning calorimetry. The thermal denaturation midpoint is effectively modulated by the addition of a suite of anions and follows the Hofmeister series. The maximum increase in thermostability (corresponding to 14 °C) was observed in the presence of 1 M sodium sulfate. After conversion of the experimental data into the change in the virial coefficient, a mechanistic model was used to estimate the relative contributions from excluded volume and preferential anion solvation for each anion. As expected, the excluded volume term stabilizes the native conformation of ProtL for all the cosolutes, but opposite effects on protein stability arise from the anion's solvation depending on their tendency to interact with or to become excluded from the protein surface. This behavior is in agreement with the results of independent NMR experiments: the anions that strongly interact with the protein surface produce significant perturbations in the amide protein chemical shift (Δd_{23}^{HN}). A correlation obtained between Δd_{23}^{HN} and the temperature coefficients for the different amide protons provides qualitative information about the structural determinants for the interaction between the protein surface and the cosolute.

Cosolutes present in the highly crowded cell environment drastically affect the constitutive properties of the solvent and ultimately its effect on protein stability. Pioneering works by Hofmeister and others underlined the influence of inorganic salts on protein solubility (*1*, *2*) and stability (*3*), ranking the compounds according to their salting out properties (the Hofmeister series). According to their effect on protein stability, cosolutes can be either stabilizing (kosmotropic) or destabilizing (chaotropic). The Hofmeister effects become important at moderate to high salt concentrations (0.01 to 1 M) and cannot be explained solely by an increase in the ionic strength or by steric exclusion (crowding effects). Much effort has been made to understand protein properties in the presence of crowding agents (*4*) and osmolites (*5*) at the same time as a plethora of experimental evidence has linked many properties to the Hofmeister effects (*6*). Important theoretical and experimental contributions reported in the literature resulted in the identification of some key factors for the influence of cosolutes on protein stability, like protein−cosolute interactions and the excluded volume effect (*7*, *8*). Despite all this effort, the mechanism by which cosolutes stabilize proteins is not yet totally clear.

The early experimental characterization of cosolute effects on protein stability involved the determination of a preferential binding coefficient using high-precision densitometry (*9*), but more recently, differential scanning calorimetry (*10*) and vapor pressure osmometry (*11*) have been used, among other techniques, for the same purpose. The majority of these experimental techniques provide very valuable information about the overall system thermodynamics, although it would also be desirable to obtain complementary experimental data with higher structural resolution. Nuclear magnetic resonance is a very versatile spectroscopic technique that allows the study of macromolecules at atomic resolution. NMR has proven to be very useful in the study of water−protein interactions (*12*), and there are examples reported in the literature in which different NMR observables have been used to study weak protein−cosolute interactions (*13*−*15*).

In this contribution, we report a detailed experimental and mechanistic study of the influence of a suite of inorganic salts on protein stability, using the IGg binding domain of B1 protein L from *Streptococcus magnus* (ProtL)[1] (*16*) as a protein model. ProtL thermal unfolding has been extensively studied in the literature and shows a well-defined, reversible, two-state transition at 70.9 °C (*17*). Thermal denaturation experiments, monitored by circular dichroism, fluorescence spectroscopy, and differential scanning calorimetry, have been used to quantify the variation of the protein thermo-

† This work was financially supported by grants from the Ministerio de Educación y Ciencia (M.P.) and the Programa Ramón y Cajal (O.M.).

* To whom correspondence should be addressed: Structural Biology Unit, CIC bioGUNE, Bizkaia Technology Park, Building 801A, 48160 Derio, Spain. Phone: 34 944 061 300. Fax: 34 944 061 301. E-mail: omillet@cicbiogune.es.

‡ CIC bioGUNE.

§ Institute for Research in Biomedicine and Universitat de Barcelona.

[1] Abbreviations: ProtL, IGg binding domain of B1 Protein L; HSQC, heteronuclear single-quantum correlation.

10.1021/bi0613426 CCC: $37.00
Published on Web 12/22/2006

dynamic parameters induced by the presence of a set of inorganic salts. The combination with the cosolute chemical shift perturbation obtained by NMR spectroscopy results in a useful strategy for gaining insight into the specific mechanism by which each of the anions in the Hofmeister series exerts its effects.

MATERIALS AND METHODS

Circular Dichroism (CD) and Fluorescence Experiments. The thermal stability of ProtL has been tested in the presence of seven different anions (chloride, fluoride, nitrate, perchlorate, phosphate, sulfate, and thiocyanate), with sodium as the counterion in all cases. Conditions for protein purification and sample preparation are described elsewhere (*18*). Experiments have been monitored by circular dichroism (CD) and fluorescence spectroscopy, sampling cosolute concentrations in a range between 100 and 800 mM. CD experiments were conducted at a protein concentration of 4 μM, employing the experimental protocol detailed in ref *18*. Thermal denaturation curves monitored by fluorescence spectroscopy were collected at a concentration of 1 μM, with measuring conditions equivalent to those of the CD experiments except for the use of a 4 nm excitation bandwidth centered at 280 nm and the recording of the emission at 350 nm. In all cases, the temperature range was sufficient for a proper determination of the baselines in both the folded and unfolded states. Selected samples were measured in duplicate, changing the detection technique, to obtain estimations of the experimental error in the thermal melt determination. Refolding curves starting from the thermally denatured state were recorded to check the degree of reversibility of the ProtL unfolding process. In all cases that were tested, the CD signal was recovered up to more than 95% of the original value, indicating that ProtL unfolding is highly reversible. A two-step reversible model for ProtL unfolding is consistent with other studies reported in the literature (*16*, *17*). For the data fitting, we have employed in-house-built scripts based on the linear extrapolation method (*19*) to determine the midpoint denaturation temperature (T_m) and the unfolding enthalpy at T_m (ΔH_m).

Differential Scanning Calorimetry. Samples containing sodium nitrate (250, 500, and 750 mM) as well as control experiments in the absence of cosolute were tested by differential scanning calorimetry in a MicroCal VP-DSC microcalorimeter. For each different cosolute concentration, the calorimeter was equilibrated overnight prior to data collection. ProtL samples were at a concentration of either 150 μM (experiments in 20 mM sodium phosphate) or 250 μM (experiments with sodium nitrate). All experiments were conducted from 283 to 363 K at a scanning rate of 60 K/h. A measure of ProtL in 20 mM phosphate buffer at pH 6.0 yielded exactly the same midpoint denaturation temperature (T_m) when compared to the one obtained by CD and a very close value for the enthalpic contribution at T_m (ΔH_m; see below). The error determination in the samples with sodium nitrate was obtained from duplicates, measured in both cases by differential scanning calorimetry.

Experimental Data Analysis and Model Fitting. Equilibrium denaturation experiments with guanidinium chloride at several temperatures (278, 285, 295, 303, 310, 318, and 328 K) and the thermal denaturation data in the absence of denaturant were simultaneously fit to the Gibbs−Helmholz equation to define the temperature dependence free energy curve for ProtL (see Figure S1 of the Supporting Information for details). The resulting values for the change in heat capacity upon unfolding (ΔC_p) and for the enthalpic contribution at T_m ($\Delta H°_m$) were 877 cal mol^{-1} K^{-1} and 53 kcal/mol, respectively. The ΔC_p value is consistent with the predicted value from the change in solvent accessible area upon unfolding (*20*). Integration of the differential scanning calorimetry curve in the absence of cosolute [20 mM phosphate buffer (pH 6.0)] yielded a value of 55 kcal/mol, in very good agreement with the value obtained from the CD data analysis.

Thermal denaturation experiments at different cosolute concentrations were used to evaluate the effect of the cosolute on ProtL's T_m and ΔH_m. At each cosolute concentration, both T_m and the enthalpy contribution at T_m (ΔH_m) were determined by fitting the experimental data assuming a two-state process (*19*). For each of the different salts that were considered, the plots of ΔH_m versus T_m were linear, providing values for the apparent heat capacity change in the presence of cosolute (ΔC^*_p) and for the enthalpy at the midpoint denaturation at a concentration of 1 M of the cosolute (ΔH^{1M}_m). Plots of ΔH_m versus T_m and the ΔC^*_p values employed in the calculations are reported in the Supporting Information.

We have calculated the excluded volume terms following the detailed protocol described by Schellman (*21*), using ASC version 2.1 (*22*) and the coordinates of 2PTL (*23*) and employing the following thermochemical radii for the different anions: 1.68 Å for chloride, 1.26 Å for fluoride, 2.00 Å for nitrate, 2.25 Å for perchlorate, 2.13 Å for phosphate, 0.95 Å for sodium, 2.18 Å for sulfate, and 2.09 Å for thiocyanate. The reported excluded volume is the average of the independent determination for the 15 lowest-energy structures, and the individual results were used to obtain the error bars shown in Figure 2B. For the estimation of the unfolded state properties, we have used the method proposed in ref *21* with the upper values reported by Rose and co-workers (*24*). We have arbitrarily assigned a null contribution to the preferential solvation term ($\Sigma K'$) of the cation, following a previously described procedure (*21*). The solvent accessible area has been calculated from the high-resolution structure (2PTL) (*23*), using ASC (*22*) with a sphere radius of 1.4 Å.

NMR Experiments. All experiments were conducted in a Bruker Avance 600 MHz spectrometer, at 298 K unless otherwise indicated. NMR sample conditions were as follows: ProtL (200 μM) isotopically enriched with ^{15}N, 10% D_2O, 0.03% sodium azide in 20 mM phosphate buffer at pH 6.0, and a variable concentration of the salt being considered (0, 250, 500, 750, and 1000 mM). The chemical shifts were estimated from the two-dimensional heteronuclear single-quantum correlation spectra (^{1}H−^{15}N HSQC) by interpolation of the peak center using nmrPipe (*25*) and in-house-built scripts. Generally, the amide proton chemical shift exhibited a linear behavior with the cosolute concentration, and the slope rendered the observed anion-induced chemical shift modulation term (Δd^{obs}_{23}). An additional factor affecting equally all residues arises from the influence of the cosolute on the water chemical shift ($\Delta d^{H_2O}_{23}$). The Δ

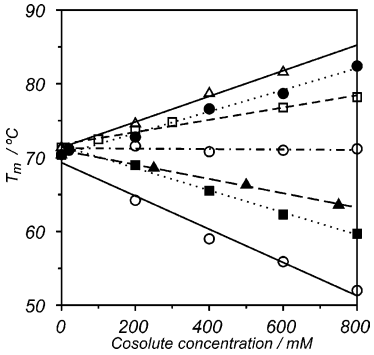

FIGURE 1: Dependence of ProtL mid-denaturation temperature (T_m) on the concentration (0−800 mM) of different sodium salts: sulfate (△, solid line), phosphate (●, dotted line), fluoride (□, dashed line), chloride (○, dashed−dotted line), nitrate (▲, dashed line), perchlorate (■, dotted line), and thiocyanate (○, solid line). The T_m values correspond to the mean values of the two independent techniques (circular dichroism and fluorescence spectroscopy) except for the sodium nitrate case, where differential scanning calorimetry alone was used. The average differences between two duplicate measurements are 0.74 (sulfate), 0.28 (phosphate), 0.42 (fluoride), 0.28 (chloride), 0.42 (nitrate), 0.84 (perchlorate), and 1.13 °C (thiocyanate).

$d_{23}^{H_2O}$ term was independently determined with samples containing 1,4-dioxane as the internal reference, and it was found to be significant for all salts but sodium fluoride. The salt-induced change in the chemical shift experienced by each amide proton (Δd_{23}^{HN}) can then be calculated from the following expression:

$$\Delta d_{23}^{HN} = \Delta d_{23}^{obs} - \Delta d_{23}^{H_2O} \quad (1)$$

For the determination of the temperature coefficients, $^1H-^{15}N$ HSQC spectra were recorded in the absence of cosolute at five different temperatures: 278, 288, 298, 308, and 318 K. The temperature coefficients were determined from the slopes obtained from the linear fits of the temperature dependencies of the chemical shift. The reported Δd_2^T values correspond to the measured data minus a constant value (9.95 ppb/K) that accounts for the water chemical shift variation with temperature. A second set of temperature coefficients were recorded in the presence of 1 M sodium thiocyanate, rendering equivalent results (see Figure S2 of the Supporting Information).

RESULTS AND DISCUSSION

Mechanistic Analysis of the Effect of Kosmotropic and Chaotropic Anions on ProtL Stability. To investigate the mechanism by which cosolutes modulate protein stability, we have expanded previously published work with sodium phosphate and sodium chloride (*18*) by measuring the changes in ProtL thermal midpoint denaturation (T_m) induced by the presence of five additional inorganic anions: sulfate, fluoride, nitrate, thiocyanate, and perchlorate, all in the form of sodium salts. Thermal denaturation curves were monitored by fluorescence spectroscopy and circular dichroism except for the nitrate anion where, due to strong background absorption, differential scanning calorimetry was used instead. For all the ions that were studied, we obtained linear dependencies between the salt concentration and T_m, with varying m_{23} slopes (Figure 1). We employ the Scatchard terminology that designates 1 to water, 2 to the protein, and 3 to the added cosolute (*26*). The nearly zero slope obtained with sodium chloride excludes an electrostatic mechanism derived from an increase in the ionic strength. Instead, the observed stabilizing effects are highly ion dependent and follow the Hofmeister series (sulfate > phosphate > fluoride > chloride > nitrate > perchlorate > thiocyanate) (*1*). The linear behavior observed with the cosolute molar concentration is also a good indicator of the existence of Hofmeister effects (*6*, *27*, *28*).

We have estimated the contribution to the free energy of unfolding induced by the presence of 1 M cosolute (at the melting temperature in the absence of cosolute, $T_m°$) using the Gibbs−Helmholtz equation (*29*, *30*):

$$\Delta G_2^{1M}(T°_m) = \Delta H_m^{1M}\left(1 - \frac{T°_m}{T_m^{1M}}\right) - \Delta C^*_p\left[(T_m^{1M} - T°_m) + T°_m \ln\left(\frac{T°_m}{T_m^{1M}}\right)\right] \quad (2)$$

where T_m^{1M} and ΔH_m^{1M} are the melting temperature and enthalpy in the presence of 1 M cosolute, respectively, and ΔC^*_p is the apparent heat capacity change in the presence of the cosolute, all of them calculated from experimental data (see Materials and Methods for details).

At this point, we have employed the linear extrapolation model (LEM) (*31*), which assumes a linear dependence of the free energy of unfolding with the cosolute concentration. LEM approximation has proven useful in the thermodynamic analysis of several proteins (*32*, *33*), and it is consistent with the observed linear dependencies between ΔH_m and the cosolute concentration in ProtL (data not shown). Under these conditions, the variation of the free energy of unfolding with the cosolute concentration ($\partial\Delta G_2/\partial C_3$) is equivalent to $\Delta G_2^{1M}(T°_m)$ since the free energy in the absence of a cosolute [$\Delta G°_2(T°_m)$] is zero by definition. Thus, changes in the second virial coefficient, ΔB_{23}, for the unfolding process can be calculated according to the following expression (*20*, *34*):

$$\Delta B_{23} = \frac{1}{RT°_m}\left(\frac{\partial \Delta G_2}{\partial C_3}\right) = \frac{\Delta G_2^{1M}(T°_m)}{RT°_m} \quad (3)$$

Figure 2A shows a histogram with the estimated values of ΔB_{23} for the different cosolutes. Theses values decrease with an increase in the chaotropic tendency of the anion. Different models for rationalizing virial coefficients have been suggested. Some of the models differentiate a local domain with characteristic thermodynamic (*11*, *35*) and dynamic (*36*) properties. This strategy, after including the exposed surface area (*20*), has been successfully employed for the interpretation of the slope in the equilibrium denaturation experiments with guanidinium chloride and urea (*37*). Alternatively, models based on changes in solvent surface tension (*38*), electrostatic models of the Hofmeister effect (*39*, *40*), expanded electrostatic models including dispersion forces (*41*), and group transfer free energy models in the presence of osmolites (*42*, *43*) have also been described. In most of the models mentioned above, competition between water and cosolute for weak binding to surface loci (preferential anion solvation) (*44*) is assumed. However, it has also been suggested that steric repulsions between

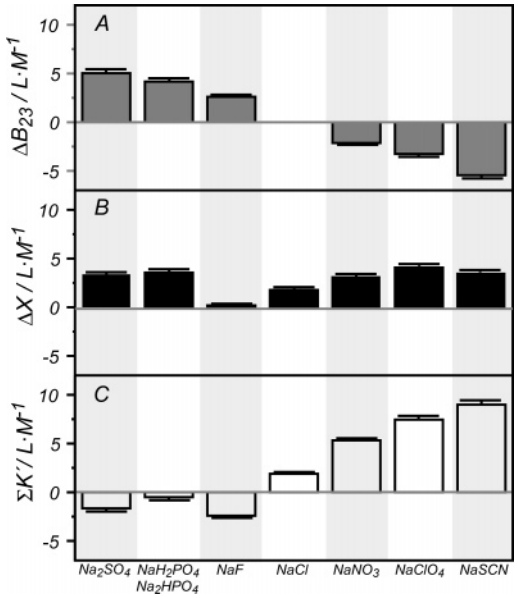

FIGURE 2: Results of thermodynamic data conversion and model analysis for the different anions: (A) changes in the second virial coefficient upon unfolding (ΔB_{23}), (B) calculated excluded volume (ΔX), and (C) preferential anion solvation ($\Sigma K'$). Errors are obtained from the propagation of the experimental error (A), the standard deviation from the independent results obtained for the 15 lowest-energy structures (B), and the propagation of the error in eq 4 (C).

solute and cosolute (excluded volume effect) may be large, and it should also be taken into consideration (*45*, *46*). Theoretical approaches have been proposed to combine both effects in a quantitative description of the effects of osmolites on protein stability (*47*, *48*). In particular, Schellman has proposed that the virial coefficient ΔB_{23} can be considered as the difference of two contributions (*21*):

$$\Delta B_{23} = \Delta X - \sum K' \qquad (4)$$

where ΔX is the change in excluded volume upon unfolding and can be estimated from the protein structure coordinates and the cosolute properties (see Materials and Methods). $\Sigma K'$ is the contribution from the preferential interaction of the cosolute with the protein with respect to water, and it is obtained from eq 4. For the suite of anions that were considered, panels B and C of Figure 2 report the determined values for ΔX and $\Sigma K'$, respectively. ΔX contributions are large and positive for all the anions, stabilizing the protein due to the smaller volume of the folded conformation. Variations among the ΔX values for the different salts reflect their distinct radii.

According to our model analysis, sulfate and phosphate anions present a negative value for the $\Sigma K'$ term, indicating a certain degree of preferential exclusion from the protein surface. In the model presented here, it is not possible to disentangle the contribution of the anion and the cation from $\Sigma K'$ (see Materials and Methods), introducing an inaccuracy in the determination of $\Sigma K'$ that affects more severely the salts with a cation-to-anion concentration ratio of >1 (phosphate and sulfate at pH 6.0). However, inspection of Figure 2 indicates that steric repulsion between solute and cosolute constitutes the main contributor to the observed changes in ProtL stability in both anions, in agreement with the proposed mechanism for the stabilization of yeast ferrocytochrome *c* by a set of oligosaccharides (*47*). Nitrate, thiocyanate, and perchlorate operate as destabilizing agents because the preferential solvation contributions for these ions ($\Sigma K'$) largely exceed their excluded volume terms, in a mechanism equivalent to the one proposed for classic denaturants like urea or guanidinium chloride (*21*). The chloride anion has a very weak effect on ProtL stability, attributed to a large compensation of the two contributions.

Changes in the second virial coefficients (ΔB_{23}) show a monotonic decay when anions are ordered following the Hofmeister series (Figure 2A). Nevertheless, our model analysis indicates that this simplicity is apparent, arising from the combination of two terms, each of them with a characteristic dependence on the position in the series. The model succeeded in attributing large contributions to the preferential solvation term for destabilizing anions, a concept suggested by many authors in the literature (*8*, *44*). Both terms, excluded volume and preferential anion solvation, reflect the nonidealities of the solution embraced in the virial coefficient, altering the properties and the composition of the solvent layers surrounding the protein and ultimately affecting its intrinsic stability.

Chemical Shift Perturbation and the Anion's Preferential Solvation. Results shown in the previous section allow discrimination of the anions according to their tendency to become accumulated in ($\Sigma K' > 0$) or excluded from ($\Sigma K' < 0$) the protein surface. The preferential solvation contribution accounts for the relative population of cosolute molecules in the protein−solvent interface. Since the chemical shift is a property sensitive to changes in the local environment, we have employed high-resolution NMR to evaluate the effects of the inorganic salts on a per residue basis, using the changes in the amide proton chemical shift as the experimental observable. Heteronuclear correlation experiments (^{1}H−^{15}N HSQC) were conducted at five different salt concentrations (0, 250, 500, 750, and 1000 mM), for each of the seven cosolutes that were considered. Figure 3 shows an overlay of spectra recorded in the presence of increasing concentrations of two representative inorganic salts: sodium sulfate (kosmotrope) and sodium thiocyanate (chaotrope). Aligned peaks are observed in the overlay of spectra, a strong indication that a single mechanism may be responsible for the chemical shift modulations. Results shown in Figure 3 are extensive to all the salts considered in this study, producing measurable changes in the chemical shift for the vast majority of the amide groups of the protein.

For a given residue, the chemical shift was found to vary linearly with salt over the whole concentration range, with no evidence of saturation. The corresponding slopes (Δd_{23}^{HN}; see Materials and Methods for details) are shown in Figure 4 for each amide proton in ProtL. Most of the chemical shift perturbations are measurable but small, consistent with the idea that the interaction between the cosolute and the protein surface is characterized by a weak binding. Inspection of Figure 4 shows that an important number of the chemical shift perturbations (including the majority of the large changes) are positive. Although it is difficult to rationalize the chemical shift perturbations, a cosolute-induced deshielding of the proton would be consistent with a transient interaction, e.g., via a hydrogen bond, with the anion. Perchlorate and thiocyanate, which induce a large number

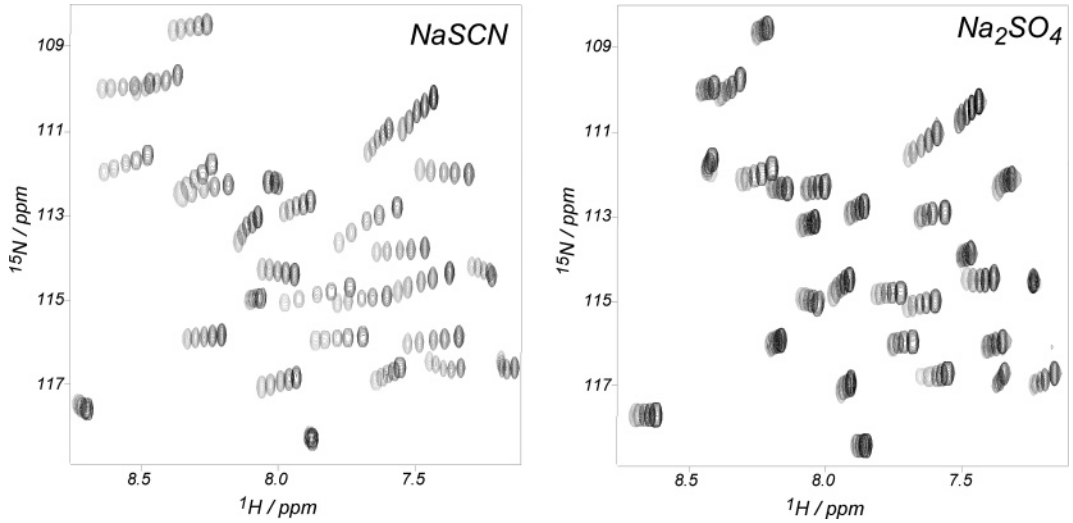

FIGURE 3: Expansion of a region in the $^{1}H-^{15}N$ HSQC spectrum of ProtL in the presence of increasing concentrations of two representative cosolutes: sodium thiocyanate and sodium sulfate. The overlay of the spectra covers the cosolute range from no added salt (black) to 1 M salt (lightest gray) with intermediate points corresponding to salt concentrations of 250, 500, and 750 mM.

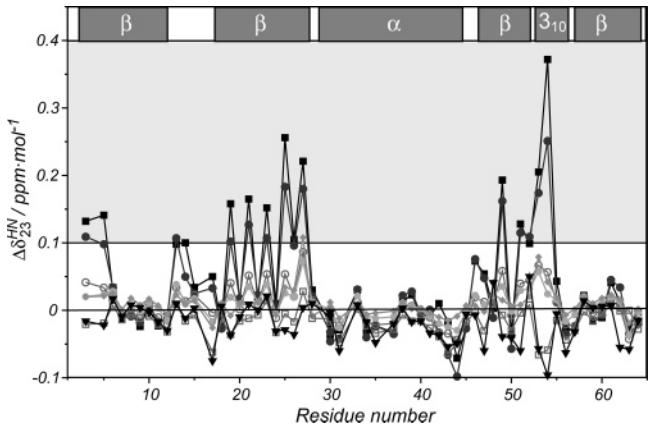

FIGURE 4: Representation of Δd_{23}^{HN} values for the different residues of ProtL in the presence of the seven cosolutes that were considered: chloride, 35% gray circles; fluoride, black triangles; nitrate, white circles; perchlorate, black squares; phosphate, white squares; sulfate, 45% gray diamonds; and thiocyanate, 85% gray circles. The area corresponding to Δd_{23}^{HN} values of >0.1 ppm has been highlighted. The secondary structure of the protein is represented at the top of the figure (α, α-helix; *β*, *β*-sheet; and 3_{10}, 3_{10}-helix).

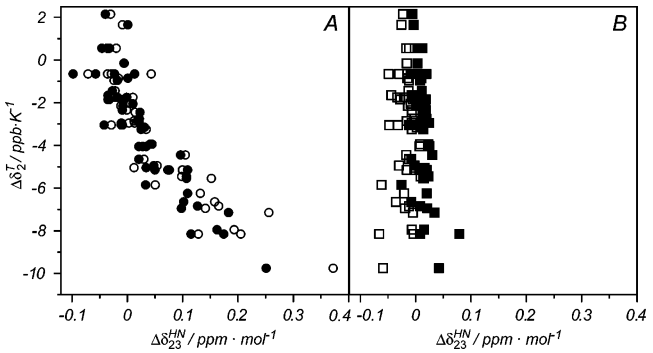

FIGURE 5: Correlation obtained between the induced chemical shift perturbation (Δd_{23}^{HN}) and the temperature coefficient (Δd_2^T) for ProtL in the presence of (A) chaotropic cosolutes sodium perchlorate (○) and sodium thiocyanate (●) and (B) kosmotropic cosolutes sodium sulfate (■) and sodium phosphate (□).

of positive shifts exceeding 0.1 ppm/mol (gray area), display the largest values of $\Sigma K'$.

Amide protons displaying the most prominent cosolvent-induced shifts are mainly associated with specific secondary structure elements and in the case of the second *β*-sheet are clearly associated with one of the sides. However, no correlation has been found with the solvent accessible area for the amide proton, indicating that the cosolute-induced chemical shift perturbation is not related to the exposed area and is more likely connected to the bonding properties of the involved hydrogen bond. Local variations in hydrogen bond length and strength associated with secondary structure elements can often be detected by measuring amide proton temperature coefficients, Δd_2^T (*49*−*51*). Temperature coefficients reflect the strength of the intramolecular hydrogen bond involved (*52*): a large (small) value for Δd_2^T corresponds to a weak (strong) hydrogen bond for the amide proton under consideration.

Figure 5A shows a good correlation between the salt-induced (Δd_{23}^{HN}) and temperature-induced (Δd_2^T) chemical shift perturbations for perchlorate and thiocyanate: the more negative the Δd_2^T, the more positive the corresponding Δd_{23}^{HN} value. According to the most widespread interpretation for the temperature coefficients (*52*), correlation in Figure 5A reveals that amide protons involved in weaker hydrogen bonds are more prone to interacting with the cosolute and vice versa. These results suggest that both Δd_{23}^{HN} and Δd_2^T are related to the bonding characteristics of the amide proton, providing a qualitative model for the interaction between the amide proton and the anion in the protein surface. To compare with kosmotropic anions, Figure 5B shows the same correlation for sulfate and phosphate. Inspection of Figure 5B clearly shows that the chemical shifts induced by these anions are too small to disclose any correlation with the temperature coefficients.

In summary, we report a comprehensive analysis of the effect of the anion Hofmeister series on protein stability. Our results show that both mechanisms suggested in the literature (excluded volume effects and preferential interactions) are active in modulating ProtL stability. The inferred values of $\Sigma K'$ are consistent with the corresponding Δd_{23}^{HN} data, particularly for the anions that exhibit a higher degree of

preferential solvation (perchlorate and thiocyanate). The correlation between Δd_{23}^{HN} and Δd_2^T in ProtL provides insight into the differences between the residues among the surface that interact with the cosolute.

ACKNOWLEDGMENT

We are very grateful to Prof. Francesc Sagués (Department de Química Física, Universitat de Barcelona) and Dr. Karin Kloiber (Vienna Biozentrum, Vienna, Austria) for helpful discussions.

SUPPORTING INFORMATION AVAILABLE

ProtL unfolding free energy as a function of temperature (Figure S1), comparison between the $\Delta\delta_2^T$ values obtained when no cosolute has been added and in the presence of 1 M sodium thiocyanate (Figure S2), and representation of the obtained values for T_m and ΔH_m at the different concentrations that were tested, for each cosolute (Figure S3). This material is available free of charge via the Internet at http://pubs.acs.org.

REFERENCES

1. Hofmeister, F. (1888) Zur lehre der Wirkung der Salze. Zweite Mittheilung, *Arch. Exp. Pathol. Pharmakol. 24*, 247−260.
2. Setchenow, J. (1889) Über die Konstitution der Salzlösungen auf Grund ihres Verhaltens zu Kohlensäure, *Z. Phys. Chem. 4*, 117−125.
3. von Hippel, P. H., and Wong, K. Y. (1964) Neutral salts. Generality of their effect on stability of macromolecular conformations, *Science 145*, 577−580.
4. Minton, A. P. (2005) Influence of macromolecular crowding upon the stability and state of association of proteins: Predictions and observations, *J. Pharm. Sci. 94*, 1668−1675.
5. Cacace, M. G., Landau, E. M., and Ramsden, J. J. (1997) The Hofmeister effect. Salt and solvent efects on interfacial phenomena, *Q. Rev. Biophys. 30*, 241−277.
6. Collins, K. D., and Washabaugh, M. W. (1985) The Hofmeister effect and the behavior of water at interfaces, *Q. Rev. Biophys. 18*, 323−422.
7. Timasheff, S. N. (2002) Protein solvent preferential interactions, protein hydration, and the modulation of biochemical reactions by solvent components, *Proc. Natl. Acad. Sci. U.S.A. 99*, 9721−9726.
8. Record, M. T., Zhang, W., and Anderson, C. F. (1998) Analysis of effects of salts and uncharged solutes on protein and nucleic acid equilibria and processes: A practical guide to recognizing and interpreting polyelectrolite effects, Hofmeister effects and osmotic effects of salts, *Adv. Protein Chem. 51*, 281−353.
9. Casassa, E. F., and Eisenberg, H. (1964) Thermodynamic analysis of multicomponent solutions, *Adv. Protein Chem. 19*, 287−395.
10. Mande, S. C., and Sobhia, M. E. (2000) Structural characterization of protein denaturant interactions: Crystal structures of hen egg white lysozyme in complex with DMSO and guanidinium chloride, *Protein Eng. 13*, 133−141.
11. Courtenay, E. S., Capp, M. W., Anderson, C. F., and Record, M. T. (2000) Vapor pressure osmometry studies of osmolyte-protein interactions: Implications for the action of osmoprotectants in vivo and for the interpretation of "osmotic stress" experiments in vitro, *Biochemistry 39*, 4455−4471.
12. Huang, H., and Melacini, G. (2006) High resolution protein hydration NMR experiments: Probing how protein surfaces interact with water and other non-covalent ligands, *Anal. Chim. Acta 564*, 1−9.
13. Jolivart, C., Böckmann, A., Riès-Kautt, M., Ducruix, A., and Guittet, E. (1998) Characterization of the interaction between bovine pancreatic trypsin inhibitor and thiocyanate by NMR, *Biophys. Chem. 71*, 221−234.
14. Foord, R. L., and Leatherbarrow, R. J. (1998) Effect of osmolytes on the exchange rates of backbone amide protons in proteins, *Biochemistry 37*, 2969−2978.
15. Jaravine, V. A., Rathgeb-Szabo, K., and Alexandrescu, A. T. (2000) Microscopic stability of cold shock protein A examined by NMR native state hydrogen exchange as a function of urea and trimethylamine N-oxide, *Protein Sci. 9*, 290−301.
16. Kim, D. E., Fischer, C., and Baker, D. (2000) A breakdown of symmetry in the folding transition state of protein L, *J. Mol. Biol. 298*, 971−984.
17. Scalley, M. L., Yi, Q., Gu, H., McCormack, A., Yates, J. R., and Baker, D. (1997) Kinetics of folding of the IgG binding domain of prptostreptoccocal Protein L, *Biochemistry 36*, 3373−3382.
18. Fayos, R., Pons, M., and Millet, O. (2005) On the origin of protein thermostabilization induced by sodium phosphate, *J. Am. Chem. Soc. 127*, 9690−9691.
19. Santoro, M. M., and Bolen, D. W. (1988) Unfolding Free Energy Changes Determined by the Linear Extrapolation Method. Denaturants? 1. Unfolding of Phenylmethanesulfonyl α-Chymotrypsin Using Different denaturants, *Biochemistry 27*, 8063−8068.
20. Myers, J. K., Pace, C. N., and Scholtz, J. N. (1995) Denaturant m values and heat capacity changes. Relation to changes in accessible surface areas of protein unfolding, *Protein Sci. 4*, 2138−2148.
21. Schellman, J. A. (2003) Protein stability in mixed solvents: A balance of contact interaction and excluded volume, *Biophys. J. 85*, 108−125.
22. Eisenhaber, F., Lijnzaad, P., Argos, P., Sander, C., and Scharf, M. (1995) The double cubic lattice method. Efficient approaches to numerical integration of surface area and volume and to dot surface contouring of molecular assemblies, *J. Comput. Chem. 16*, 273−284.
23. Wikstrom, M., Drakenberg, T., Forsen, S., Sjobrink, U., and Bjorck, L. (1994) 3-dimensional solution structure of an inmunoglobulin light chain binding domain of protein L. Comparison with the IgG binding domains of protein G, *Biochemistry 33*, 14011−14017.
24. Creamer, T. P., Srinivasan, R., and Rose, G. D. (1997) Modeling unfolded states of proteins and peptides. 2. Backbone solvent accessibility, *Biochemistry 36*, 2832−2835.
25. Delaglio, F., Grzesiek, S., Vuister, G. W., Zhu, G., Pfeifer, J., and Bax, A. (1995) NMRPipe: A multidimensional spectral processing system based on UNIX pipes, *J. Biomol. NMR 6*, 277−293.
26. Scatchard, G. (1946) Physical chemistry of protein solutions. 1. Derivation of the equations for the osmotic pressure, *J. Am. Chem. Soc. 68*, 2315−2319.
27. von Hippel, P. H., and Wong, K. Y. (1962) Effect of ions on kinetics of formation and stability of collagen fold, *Biochemistry 1*, 664−674.
28. Baldwin, R. L. (1996) How Hofmeister ion interactions affect protein stability, *Biophys. J. 71*, 2056−2063.
29. Santoro, M. M., Liu, Y., Khan, S. M. A., Hou, L., and Bolen, D. W. (1992) Increased thermal stability of proteins in the presence of naturally occurring osmolytes, *Biochemistry 31*, 5278−5283.
30. Becktel, W. J., and Schellman, J. A. (1987) Protein stability curves, *Biopolymers 26*, 1859−1877.
31. Schellman, J. A. (1978) Solvent denaturation, *Biopolymers 17*, 1305−1322.
32. Naik, N. T., and Huang, T. (2004) Conformational stability and thermodynamic characterization of the lipoic acid bearing domain of human mitochondrial branched chain α-ketoacid dehydrogenase, *Protein Sci. 13*, 2483−2492.
33. Reddy, G. B., Purnapatre, K., Lawrence, R., Roy, S., Varshney, U., and Surolia, A. (1999) Linear free-energy model description of the conformational stability of uracil-DNA glycosylase inhibitor: A thermodynamic characterization of interaction with denaturant and cold denaturation, *Eur. J. Biochem. 261*, 610−617.
34. David-searles, P. R., Saunders, A. J., Erie, D. A., Winzor, D. J., and Pielak, G. J. (2001) Interpreting the effects of small uncharged solutes on protein folding equilibria, *Annu. Rev. Biophys. Biomol. Struct. 30*, 271−306.
35. Lee, J. C., and Timasheff, S. N. (1974) Partial specific volumes and interactions with solvent components of proteins in guanidine hydrochloride, *Biochemistry 13*, 257−265.
36. Schellman, J. A. (1990) A simple model for solvation in mixed solvents. Aplications to the stabilization and destabilization of macromolecualr structures, *Biophys. Chem. 37*, 121−140.
37. Courtenay, E. S., Capp, M. W., Saeker, R. M., and Record, M. T. (2000) Thermodynamic analysis of interactions between denaturants and protein surface exposed on unfolding: Interpretation of urea and guanidinium chloride m values and their correlation with changes in accessible surface area (ASA) using preferential

interaction coefficients and the local-bulk domain model, *Proteins Suppl. 4*, 72−85.
38. Arakawa, T., and Timasheff, S. N. (1982) Stabilization of protein structure by sugars, *Biochemistry 21*, 6536−6544.
39. Zhou, H. X. (2005) Interactions of macromolecules with salt anions: An electrostatic theory for the Hofmeister effect, *Proteins 61*, 69−78.
40. Boström, M., Kunz, W., and Ninham, B. W. (2005) Hofmeister effects in surface tension of aqueous electrolyte solution, *Langmuir 21*, 2619−2623.
41. Kunz, W., Lo Nostro, P., and Ninham, B. W. (2004) The present state of affairs with Hofmeister effects, *Curr. Opin. Colloid Interface Sci. 9*, 1−18.
42. Auton, M., and Bolen, D. W. (2005) Predicting the energetics of osmolyte-induced protein folding/unfolding, *Proc. Natl. Acad. Sci. U.S.A. 102*, 15065−15068.
43. Auton, M., and Bolen, D. W. (2004) Additive transfer free energies of the peptide backbone unit that are independent of the model compound and the choice of concentration scale, *Biochemistry 43*, 1329−1342.
44. Timasheff, S. N. (1998) Control of protein stability and reactions by weakly interacting cosolvents: The simplicity of the complicated, *Adv. Protein Chem. 51*, 355−432.
45. Colonna-Cesan, F., and Sander, C. (1990) Excluded volume approximation to protein-solvent interaction. The solvent contact model, *Biophys. J. 57*, 1103−1107.
46. Wills, P. R., Hall, D. R., and Winzor, D. J. (2000) Interpretation of the thermodynamic non-ideality in sedimentation equilibrium experiments on proteins, *Biophys. Chem. 84*, 217−225.
47. Saunders, A. J., Davis-Searles, P. R., Allen, D., Pielak, G., and Erie, D. A. (2000) Osmolyte induced changes in protein conformation equilibria, *Biopolymers 53*, 293−307.
48. Shimizu, S., and Smith, D. J. (2004) Preferential hydration and the exclusion of cosolvents from protein surfaces, *J. Chem. Phys. 121*, 1148−1154.
49. Baxter, N. J., and Williamson, M. P. (1997) Temperature dependence of H-1 chemical shifts in proteins, *J. Biomol. NMR 9*, 359−369.
50. Andersen, N. H., Neidigh, J. W., Harris, S. M., Lee, G. M., Liu, Z., and Tong, H. (1997) Extracting information from the temperature gradients of polypeptide NH chemical shifts. 1. The importance of conformational averaging, *J. Am. Chem. Soc. 119*, 8547−8561.
51. Contreras, M. A., Haack, T., Royo, M., Giralt, E., and Pons, M. (1997) Temperature coefficients of peptides dissolved in hexafluoroisopropanol monitor distortions of helices, *Lett. Pept. Sci. 4*, 29−39.
52. Cierpicki, T., and Otlewski, J. (2001) Amide proton temperature coefficients as hydrogen bond indicators in proteins, *J. Biomol. NMR 21*, 249−261.

BI0613426